Supplementary Figures, Table, and Methods for:

Multi-modal optical sensing and analyte specificity via single-walled carbon nanotubes

Daniel A. Heller[1], Hong Jin[1], Brittany M. Martinez[1,†], Dhaval Patel[1,‡], Brigid M. Miller[1], Tsun-Kwan Yeung[1,§], Prakrit V. Jena[2], Claudia Höbartner[3,¶], Taekjip Ha[2,4,5], Scott K. Silverman[3], and Michael S. Strano[1,*]

[1]Department of Chemical Engineering, Massachusetts Institute of Technology, Cambridge, MA 02139, USA

[2]Department of Physics, University of Illinois at Urbana-Champaign, Urbana, IL 61801, USA

[3]Department of Chemistry, University of Illinois at Urbana-Champaign, Urbana, IL 61801, USA

[4]Beckman Institute for Advanced Science and Technology, University of Illinois at Urbana-Champaign, Urbana, IL 61801, USA

[5]Howard Hughes Medical Institute, Urbana, IL 61801, USA

[†] Current Address: United States Patent and Trademark Office, Alexandria, VA 22314, USA

[‡] Current Address: School of Chemical & Biomolecular Engineering, Georgia Institute of Technology, Atlanta, GA 30332, USA

[§] Current Address: Department of Physics, Harvard University, Cambridge, MA 02138, USA

[¶] Current Address: Max Planck Institute for Biophysical Chemistry, 37077 Göttingen, Germany

[*]To whom correspondence should be addressed. Email: strano@mit.edu

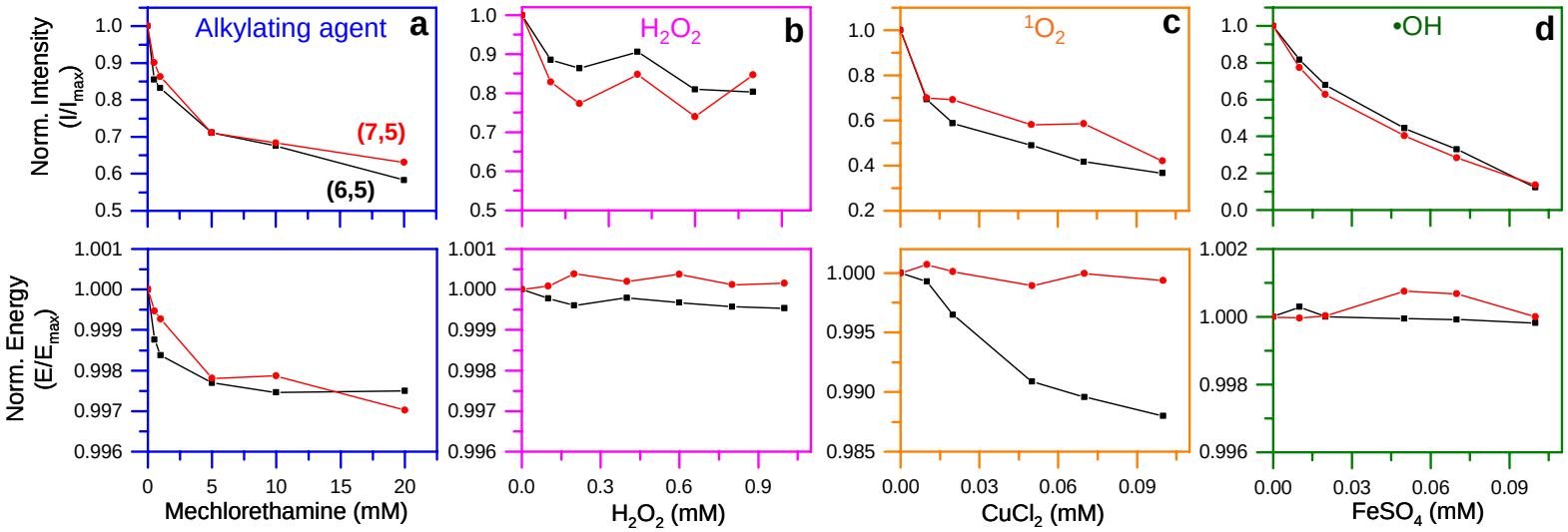

Supplementary Figure S1: Concentration dependence of SWNT response to genotoxins. Plots of (6,5) and (7,5) SWNT energy and intensity upon varying genotoxin concentrations in buffered 5 mg/L CoMoCAT SWNT solution. (**a**) Mechlorethamine response acquired 7 hours after addition. (**b**) Hydrogen peroxide response acquired 24 hours after addition. (**c**) Singlet oxygen response acquired 1 hour after addition of hydrogen peroxide. (**d**) Hydroxyl radical response acquired 10.5 hours after addition of hydrogen peroxide. Data was acquired approximately when reagent reached steady-state, with the exception of singlet oxygen due to difficulty of deconvolution of overlapping (6,5) and (7,5) bands over long reaction times.

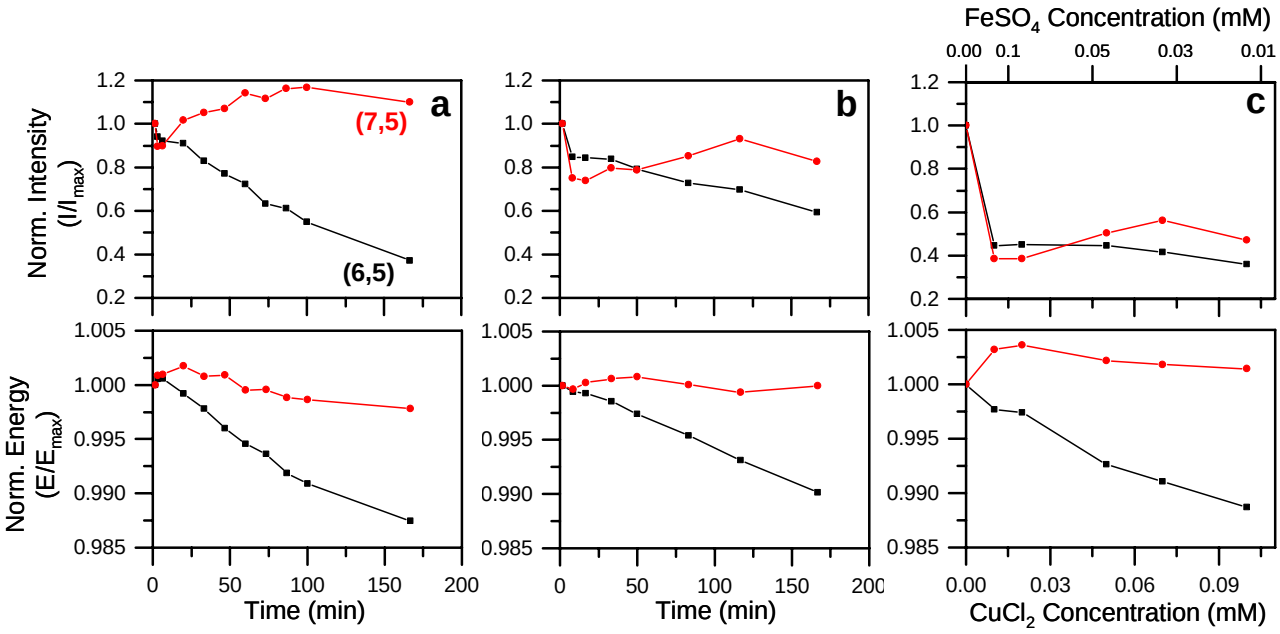

Supplementary Figure S2: Multiplexed detection of singlet oxygen and hydroxyl radicals. Plots of (6,5) and (7,5) intensity and energy upon inducing both singlet oxygen and hydroxyl radical production in the presence of 5 mg/L CoMoCAT DNA-SWNT show characteristics of both agents. With increasing $FeSO_4$/decreasing $CuCl_2$ concentration, the initial intensity drop of the (7,5) nanotube is more pronounced and remains for a longer duration. Concomitantly, the rate of (6,5) energy shift decreases. (**a**) Intensity (top) and energy (bottom) with 0.02 mM $FeSO_4$, 0.08 mM $CuCl_2$ and 10 mM H_2O_2. (**b**) 0.04 mM $FeSO_4$, 0.06 mM $CuCl_2$ and 10 mM H_2O_2. (**c**) Plots showing concentration dependence of spectral changes. Data was acquired 60 minutes after introduction of reagents. $FeSO_4$ and $CuCl_2$ concentrations were varied in compensatory fashion (with the exception of the 0,0 data point), while H_2O_2 concentration remained at 10 mM.

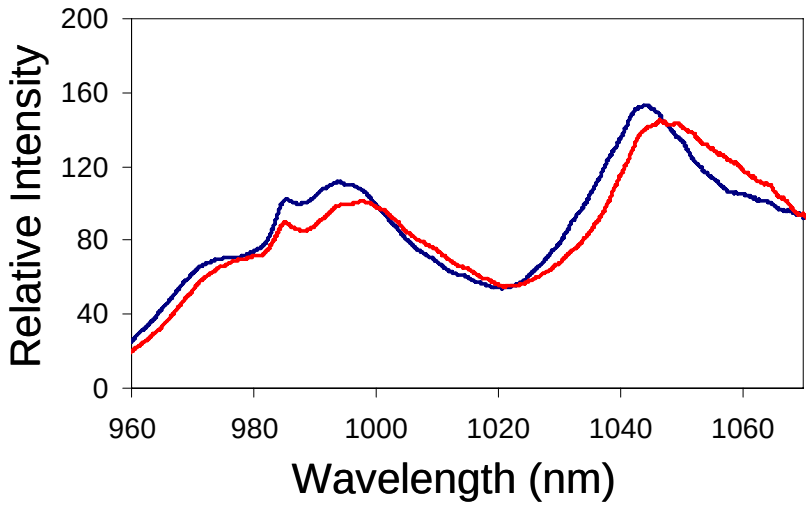

Supplementary Figure S3: Detection of chemotherapeutic drugs using HiPCO SWNT. The DNA-SWNT complex prepared using HiPCO SWNT behaved in a qualitatively similar manner to the complex fabricated with CoMoCAT SWNT. Red-shifting of both (6,5) and (7,5) SWNT species is observed upon introduction of melphalan (red) compared to the control spectrum (blue).

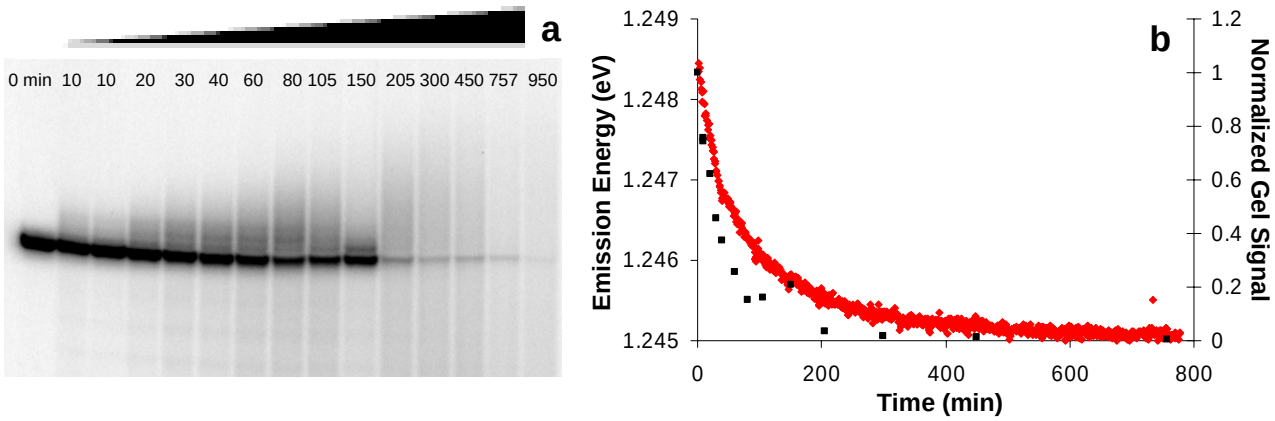

Supplementary Figure S4: Comparison between damage to free d(GT)$_{15}$ DNA and DNA-SWNT fluorescence red-shift from alkylating agent activity. (**a**) PAGE kinetic study of 0.9 mM melphalan reaction on the d(GT)$_{15}$ oligonucleotide sequence. (**b**) Normalized intensity of the remaining d(GT)$_{15}$ band from PAGE (black squares) plotted against the red-shift of d(GT)$_{15}$ encapsulated SWNT exposed to melphalan (red diamonds) under the same conditions. The d(GT)$_{15}$ oligonucleotide did not produce distinct bands in the gel due to multiple guanine damage sites, prompting the use of a test sequence containing only one guanine base (Fig. 2). The test sequence exhibits the same kinetics as shown above upon exposure to melphalan.

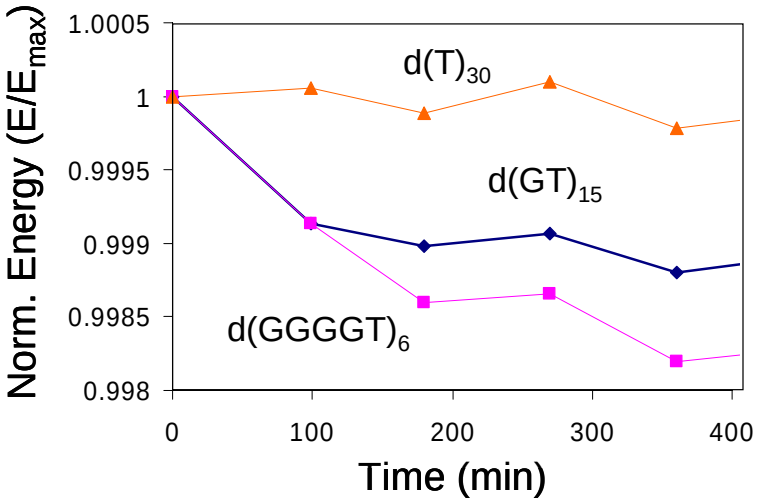

Supplementary Figure S5: Sequence dependence of alkylating agent detection by DNA-SWNT. Rate of (6,5) nanotube photoluminescence red-shift upon melphalan exposure to nanotubes encapsulated by sequences of varying G/T ratios. Nanotube-DNA complexes with sequences containing a higher fraction of guanine display higher reactivity to alkylating drugs, consistent with the observed behavior of nitrogen mustard agents[1].

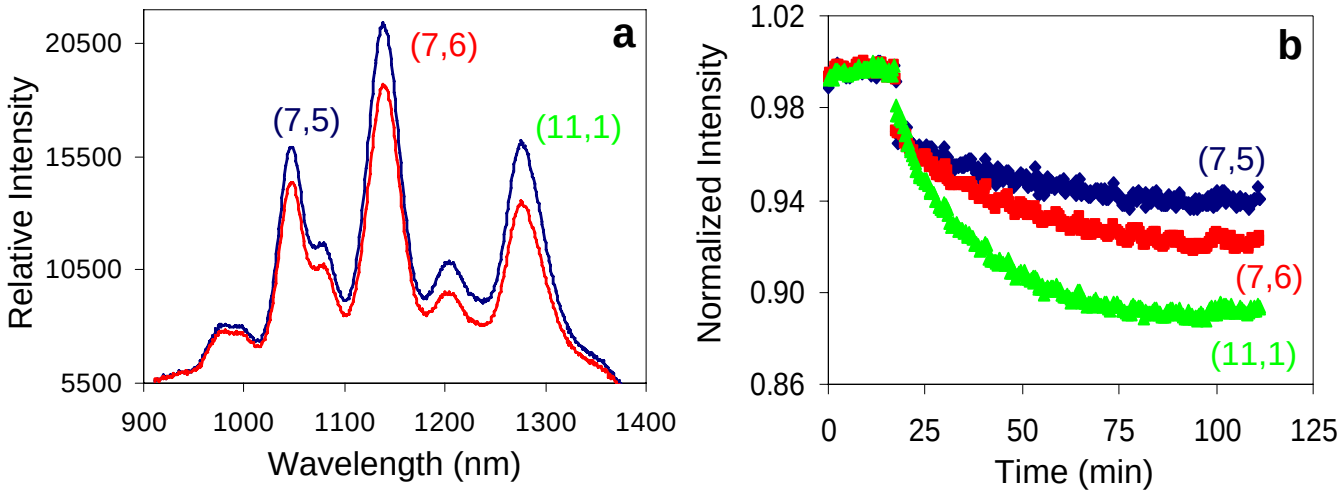

Supplementary Figure S6: Hydrogen peroxide photoluminescence quenching of DNA-SWNT. The hydrogen peroxide response of DNA-SWNT using HiPCO nanotubes excited at 633 nm demonstrates SWNT species dependence. (**a**) The spectrum taken after exposure to 10 mM H_2O_2 for 24 hours (red curve) shows greater attenuation of small bandgap nanotubes (emitting at longer wavelengths) compared to the control spectrum (blue curve). Large bandgap nanotubes (such as the (7,5) species) exhibit less attenuation. (**b**) Transient attenuation of three SWNT species showing higher rates for smaller bandgap semiconducting species. The reaction was conducted in 20 mM Tris at a pH of 7.3 with 0.1 M NaCl.

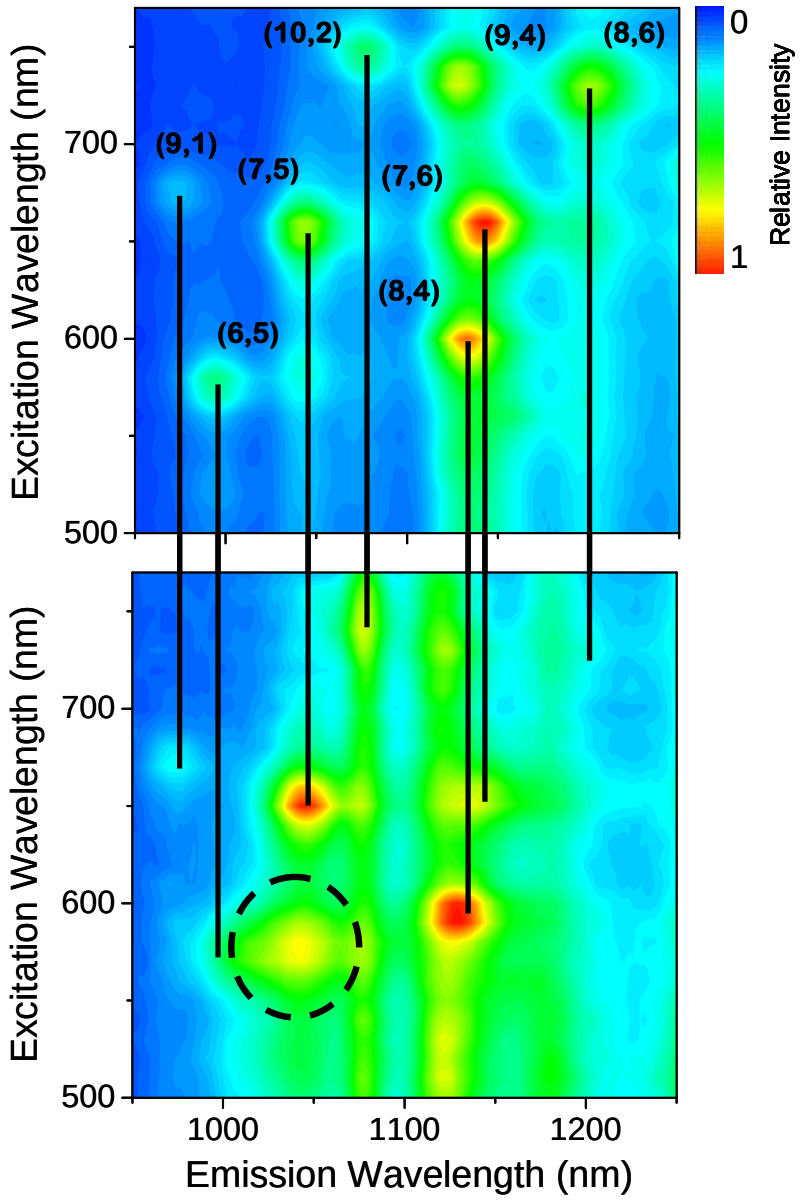

Supplementary Figure S7: Singlet oxygen reaction on HiPCO DNA-SWNT. A 3D photoluminescence profile of 5 mg/L DNA-SWNT using HiPCO nanotubes before (top) and 24 hours after (bottom) exposure to $CuCl_2$ and hydrogen peroxide in 20 mM Tris buffer with a pH of 7.3 and 0.1 M NaCl. The (6,5) nanotube undergoes a large red shift (circled in bottom trace). Relative intensity changes of nanotube species occur, and total intensity of all peaks fall, demonstrating similar behavior to CoMoCAT prepared SWNT (Fig. 2). Plot intensities were normalized independently. The CoMoCAT SWNT preparation, whose (6,5) and (7,5) relative abundances are approximately 2:1, and whose (6,5) concentration is near 40% of the total SWNT content, was chosen for most of the sensing work in this paper over the HiPCO preparation, whose approximate (6,5) and (7,5) fractional intensities are 3.7% and 4.9% respectively of the total photoluminescence in HiPCO SWNT[2, 3].

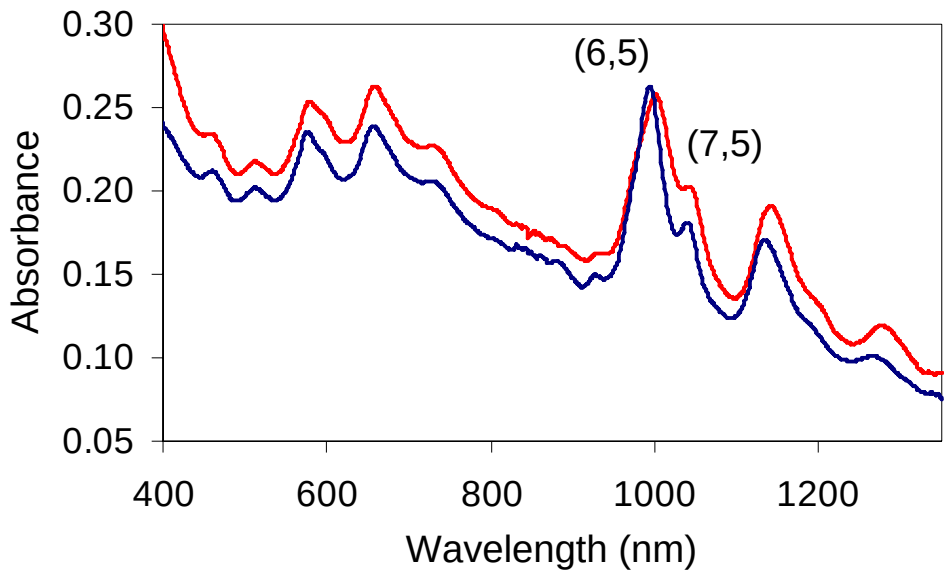

Supplementary Figure S8: Singlet oxygen shifts SWNT absorption bands. Absorption spectra of 5 mg/L d(GT)$_{15}$ encapsulated CoMoCAT SWNT before (blue) and 24 hours after (red) inducing singlet oxygen production. The (6,5) band exhibits a red-shift while the (7,5) band shows little change in wavelength. The E_{22} bands exhibit shifting to a lesser degree than E_{11} bands. The samples were buffered in 20 mM Tris at a pH of 7.3 with 0.1 M NaCl.

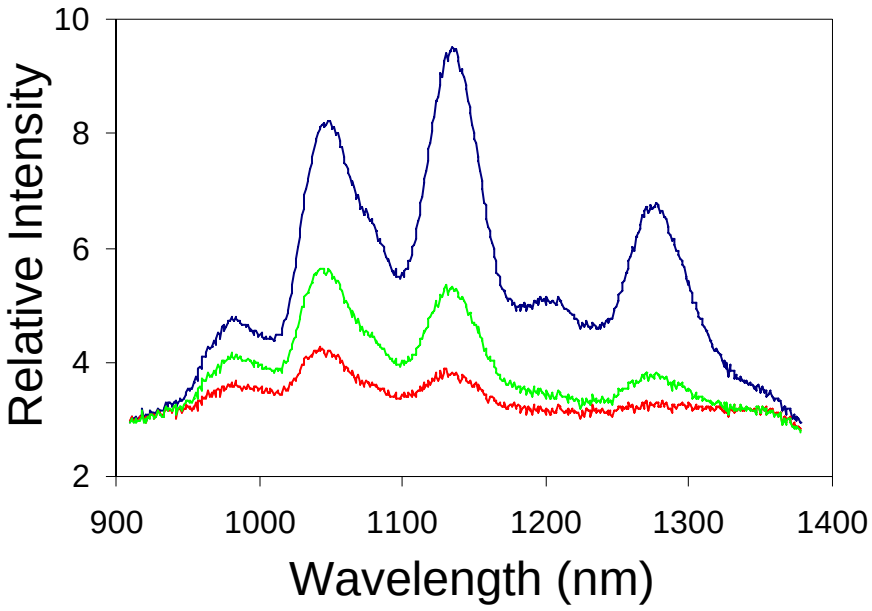

Supplementary Figure S9: Hydroxyl radical detection by DNA-SWNT. DNA-SWNT detects hydroxyl radicals by species-specific quenching. The photoluminescence quenching of smaller bandgap SWNT is highly disproportionate upon exposure of Fenton reagents to DNA-encapsulated HiPCO-SWNT (633 nm excitation).

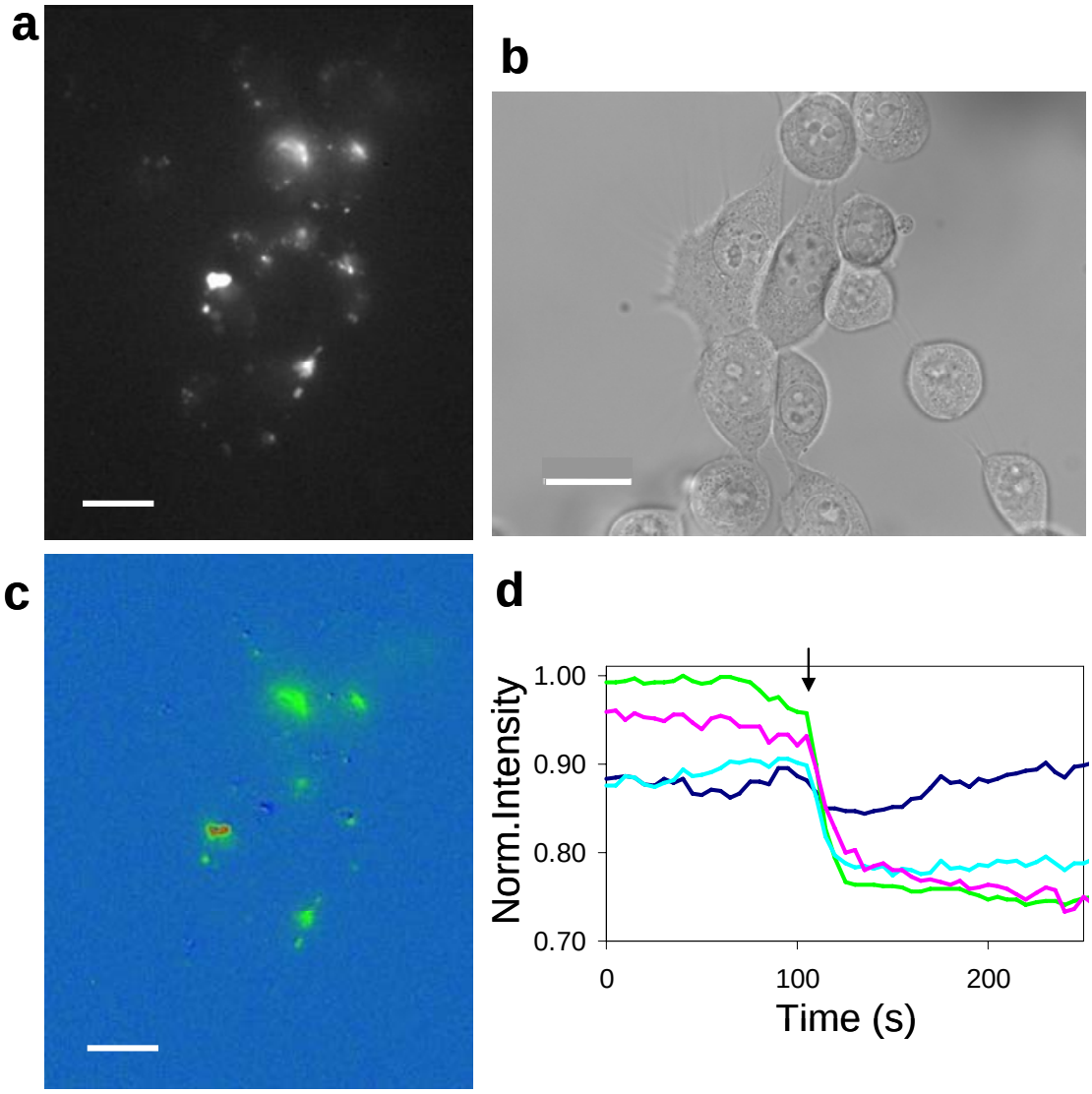

Supplementary Figure S10: Real-time imaging of hydrogen peroxide quenching in live cells. DNA-SWNT emission from 3T3 cells upon introduction of hydrogen peroxide shows inhomogeneous signal attenuation across the cell sample. (**a**) Near-infrared image of SWNT photoluminescence in 3T3 cells. (**b**) Visible image. (**c**) Subtracted near-infrared image (intensity before minus after reagent addition) shows locations where the intensity decreased after addition. Scale bars are 20 μm. (**d**) Traces of individual emitting particles demonstrate various degrees of signal attenuation. Arrow denotes time of H_2O_2 introduction. Cells were excited at 785 nm through a 63x microscope objective. An included Supplementary Video file contains the near-infrared movie of SWNT response to hydrogen peroxide.

Supplementary Table S1

Principal components analysis scores for all reagents.

		Conc. (mM) or Time (min)	PC 1	PC 2	PC 3	PC 4
Concentration (mM)	Mechlorethamine	1	-0.3115	-0.0642	0.0983	-0.0605
		5	-0.181	0.1469	0.1418	-0.074
		10	-0.1482	0.1752	0.1193	-0.061
		20	-0.1131	0.2966	0.1573	-0.0263
	H_2O_2	0.2	-0.4365	-0.0335	-0.037	-0.104
		0.6	-0.4252	0.0201	-0.0584	-0.0776
		0.8	-0.4264	-0.0428	0.0127	-0.0196
		1	-0.4064	0.0167	-0.0231	-0.0225
	Singlet oxygen	0.02	-0.0582	0.0894	-0.0842	0.0442
		0.05	0.5275	0.1143	-0.0423	-0.0078
		0.07	0.6579	0.068	-0.1408	0.0598
		0.1	0.8483	0.1908	-0.1707	-0.0127
	Hydroxyl radicals	0.02	-0.3469	0.1276	-0.0801	-0.0359
		0.05	-0.3103	0.404	-0.2477	0.06
		0.07	-0.2878	0.4868	-0.2543	0.0473
		0.1	-0.1743	0.5756	-0.3574	0.0877
	Multiplexed	0.01	-0.1296	0.2705	-0.5133	0.0585
		0.02	-0.1101	0.2433	-0.5492	0.0592
		0.05	0.3464	0.0957	-0.3726	0.0578
		0.07	0.4967	0.0458	-0.3126	0.0915
		0.1	0.7541	0.0867	-0.332	0.0594
Time (min)	Mechlorethamine	200	-0.258	0.0654	0.1541	-0.0811
		250	-0.2546	0.0829	0.1117	-0.0992
		300	-0.2339	0.086	0.1217	-0.0969
		350	-0.2303	0.1072	0.137	-0.1092
	H_2O_2	10	-0.4671	-0.2114	0.0914	-0.0799
		14	-0.4641	-0.2078	0.0877	-0.0799
		19	-0.4633	-0.2014	0.089	-0.0725
		25	-0.4633	-0.198	0.0893	-0.0752
		29	-0.4617	-0.2021	0.0847	-0.073
		32	-0.4621	-0.2032	0.0865	-0.0701
	Singlet oxygen	150	1.1962	-0.1937	0.0388	-0.1394
		200	1.4986	-0.0674	0.1048	-0.2139
		250	1.5992	0.0166	0.0704	-0.2432
		300	1.6098	0.0338	0.005	-0.2247
		350	1.618	0.0698	0.0003	-0.2176
		400	1.6362	0.0724	0.0088	-0.2097
	Hydroxyl radicals	0.6	-0.4731	0.1206	-0.1155	-0.0795
		0.9	-0.4532	0.1754	-0.125	-0.0607
		1.1	-0.4447	0.2027	-0.1335	-0.0343
		2.1	-0.4254	0.2387	-0.1629	-0.0497
	Multiplexed 0.06 mM $CuCl_2$ and 0.04 mM $FeSO_4$	8.3	-0.4028	0.0176	0.0157	-0.1169
		16.7	-0.3958	-0.003	-0.0462	-0.111
		33.3	-0.3365	-0.0776	-0.0517	-0.0774
		50.0	-0.2138	-0.0879	-0.0769	-0.0512
		83.3	-0.0093	-0.1223	0.0081	0.0034

		116.7	0.2114	-0.1922	0.1038	0.0365
		166.7	0.5266	-0.1759	-0.0105	0.0495
		250.0	0.8633	-0.2135	0.0797	0.0736
	Multiplexed 0.08 mM $CuCl_2$ and 0.02 mM $FeSO_4$	3.3	-0.5679	-0.1537	-0.014	-0.0853
		6.7	-0.5666	-0.1488	-0.0226	-0.0674
		20.0	-0.4569	-0.2969	-0.0395	0.0069
		33.3	-0.3007	-0.2752	0.054	0.0633
		46.7	-0.1198	-0.3125	0.0435	0.104
		60.0	0.0373	-0.3173	0.1939	0.146
		73.3	0.1471	-0.281	0.1634	0.1981
		86.7	0.3241	-0.3199	0.2481	0.212
		100.0	0.4315	-0.3093	0.2589	0.2532
		166.7	0.8192	-0.2291	0.279	0.315
In Vivo	Mechlorethamine	35	-0.0198	0.4806	0.304	0.2008
		40	0.1889	0.5068	0.2353	0.1775
		50	0.4151	0.5037	0.2844	0.2169
		60	0.4448	0.5714	0.3703	0.1673
	H_2O_2	5	-0.5231	-0.2088	0.0941	-0.0569
		6	-0.2878	-0.032	0.1025	-0.0258
		7	-0.3114	-0.0179	0.1011	-0.0114
		8	-0.3675	-0.0875	0.0481	-0.0279
		9	-0.4438	-0.1663	0.0577	-0.0636
		10	-0.5076	-0.2598	0.0146	-0.0853
		11	-0.4535	-0.2647	0.0844	-0.0863
		12	-0.4963	-0.2964	0.1076	-0.0641
	Singlet oxygen	11.7	-0.0765	-0.1321	-0.3959	0.1042
		16.7	0.0659	-0.1515	-0.2195	0.0714
		30.0	0.1345	-0.2305	-0.093	0.0804
		43.3	0.1714	-0.3517	-0.299	0.1306
		58.3	0.2181	-0.3444	-0.1915	0.1224
		70.0	0.2438	-0.4168	-0.1874	0.1378
		83.3	0.2461	-0.5589	-0.212	0.2212
	Hydroxyl radicals	3	-0.4632	-0.0685	-0.0172	-0.1283
		4	-0.3465	0.1997	0.0733	-0.018
		5	-0.3044	0.3222	0.1587	0.0185
		6	-0.2921	0.3311	0.1472	0.0406
		7	-0.2168	0.3361	0.2032	0.0435
		8	-0.1834	0.3718	0.1813	0.0333
		9	-0.194	0.3631	0.1632	0.0354

Supplementary Methods

Single-molecule studies

Nanotubes were encapsulated with DNA via probe-tip sonication in a 4:1 DNA:HiPCO SWNT ratio for 2 min. A ratio of 1:4 biotinylated:non-biotinylated $d(GT)_{15}$ DNA was used to produce complexes with multiple biotinylated oligonucleotides per SWNT. Solutions were centrifuged at 16,000 g for 90 minutes and the pellet was discarded. A sample chamber for single-molecule experiments was created as described[4]. The surface was successively treated with 1 mg/ml biotinylated-BSA in T100 (10 mM Tris [pH 8.0] and 0.1 M NaCl) and 0.2 mg/ml Neutravidin in T100. Biotinylated DNA-SWNT (concentration approximately 1 mg/L) in T100 was added to the sample chamber and incubated for at least 30 minutes before imaging. Channels were flushed with deionized water before imaging. Near-IR movies were captured at 1 frame/s using 633 nm excitation. An aliquot of 10 μM H_2O_2 was dropped on the inlet hole of the slide and allowed to diffuse into the sample chamber during data acquisition.

Concentration-dependent genotoxin responses

Buffered solutions of 5 mg/L GT-CoMoCAT SWNT were prepared to expose the SWNT complexes to six different concentrations of each genotoxin: mechlorethamine, H_2O_2, singlet oxygen, and hydroxyl radicals. The latter two were prepared by first adding several concentrations of $CuCl_2$ for singlet oxygen or $FeSO_4$ for hydroxyl radicals one hour before initiating the reactions with 10 mM H_2O_2. Spectra were acquired at a single time point for each genotoxin.

Multiplexed detection experiments

Solutions of 5 mg/L of GT-CoMoCAT SWNT in buffer were exposed to mixtures of $CuCl_2$ and $FeSO_4$ in several ratios. Cations were introduced to the solutions one hour before starting the reactions with 10 mM H_2O_2. Multiple near-infrared spectra were recorded on samples over a five-hour period for transient spectra, or after 1 hour of reaction time for concentration-dependent studies.

Chemotherapeutic drug detection using SWNT encapsulated in multiple DNA sequences

Solutions of 5 mg/L HiPCO SWNT were encapsulated by $d(T)_{30}$, $d(GT)_{15}$, and $d(GGGGT)_6$ via bath sonication for 1 hour in a 1:1 SWNT:DNA mass ratio. The resulting solution was centrifuged at 16,300 g for 90 minutes and the pellet was discarded. The near-infrared photoluminescence of each DNA-SWNT complex was measured upon addition of 0.9 mM melphalan in 100 mM Tris buffer (pH 7.4).

References

1. Povirk, L.F. & Shuker, D.E. DNA-Damage and Mutagenesis Induced by Nitrogen Mustards. *Mutat Res-Rev Genet* **318**, 205-226 (1994).
2. Jorio, A. et al. Quantifying carbon-nanotube species with resonance Raman scattering. *Phys Rev B* **72**, 075207 (2005).
3. Bachilo, S.M. et al. Narrow (n,m)-distribution of single-walled carbon nanotubes grown using a solid supported catalyst. *J Am Chem Soc* **125**, 11186-11187 (2003).
4. Ha, T. Single-molecule fluorescence resonance energy transfer. *Methods* **25**, 78-86 (2001).